

[3,3]-Sigmatropic Rearrangement versus Carbene Formation in Gold-Catalyzed Transformations of Alkynyl Aryl Sulfoxides: Mechanistic Studies and Expanded Reaction Scope

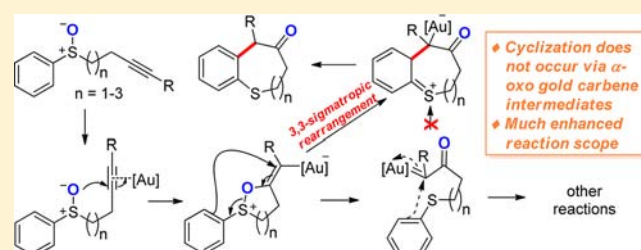
Biao Lu,^{†,#} Yuxue Li,^{*,‡} Youliang Wang,[†] Donald H. Aue,[†] Yingdong Luo,[†] and Liming Zhang^{*,†}

[†]Department of Chemistry & Biochemistry, University of California, Santa Barbara, California 93117, United States

[‡]State Key Laboratory of Organometallic Chemistry, Shanghai Institute of Organic Chemistry, Ling Ling Road 345, Shanghai 200032, China

S Supporting Information

ABSTRACT: Gold-catalyzed intramolecular oxidation of terminal alkynes with an arenesulfinyl group as the tethered oxidant is a reaction of high impact in gold chemistry, as it introduced to the field the highly valued concept of gold carbene generation via alkyne oxidation. The proposed intermediacy of α -oxo gold carbenes in these reactions, however, has never been substantiated. Detailed experimental studies suggest that the involvement of such reactive intermediates in the formation of dihydrobenzothiepinones is highly unlikely. Instead, a [3,3]-sigmatropic rearrangement of the initial cyclization intermediate offers a reaction path that can readily explain the high reaction efficiency and the lack of sulfonium formation. With internal alkyne substrates, however, the generation of a gold carbene species becomes competitive with the [3,3]-sigmatropic rearrangement. This reactive intermediate, nevertheless, does not proceed to afford the Friedel–Crafts-type cyclization product. Extensive density functional theory studies support the mechanistic conclusion that the cyclized product is formed via an intramolecular [3,3]-sigmatropic rearrangement instead of the previously proposed Friedel–Crafts-type cyclization. With the new mechanistic insight, the product scope of this versatile formation of mid-sized sulfur-containing cycloalkenones has been expanded readily to various dihydrobenzothiecinones, a tetrahydrobenzocyclononone, and even those without the entanglement of a fused benzene ring. Besides gold, Hg(OTf)₂ can be an effective catalyst, thereby offering a cheap alternative for this intramolecular redox reaction.

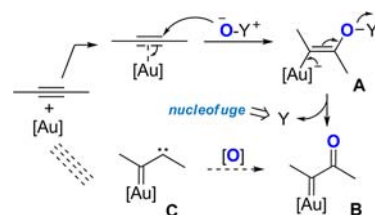


INTRODUCTION

Homogeneous gold catalysis¹ is a rather recent phenomenon but has generated tremendous interest and excitement in the synthetic community. Its explosive growth owes much to various aspects of novel and unprecedented reactivities of gold complexes and to synergistic efforts from many research groups around the world.

One particularly rewarding, and still evolving, area in gold catalysis is the oxidation of alkynes using oxygen-delivering nucleophilic oxidants.² These oxidants are composed of two parts: a negatively charged, thus nucleophilic, oxygen and a positively charged, thus potent, leaving group (nucleofuge). The gold catalysis follows the sequence outlined in Scheme 1: first, the nucleophilic oxygen from the oxidant would attack a gold-activated C–C triple bond in an *anti* addition; the alkenylgold intermediate thus formed (i.e., A) would then undergo γ -elimination, expelling the nucleofugal part of the oxidant and generating an α -oxo gold carbene intermediate (i.e., B). Since B could formally be formed through selective oxidation of the carbene center of an α -carbene gold carbene C, the overall transformation in Scheme 1 makes stable and benign alkynes in the presence of a gold complex equivalent to the

Scheme 1. Gold-Catalyzed Oxidation of Alkynes Using Oxygen-Delivering Oxidants

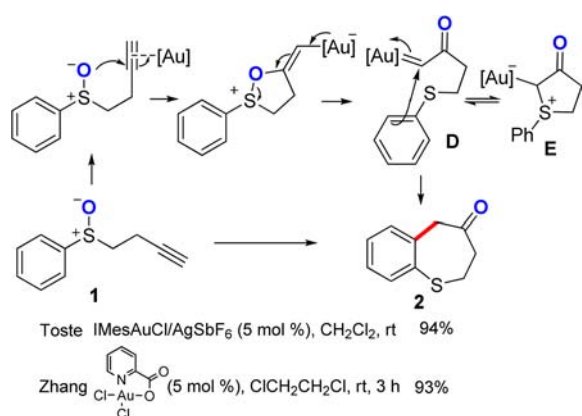


imaginary species C, offering a formal access to the reactivities of this provocative structure and foretelling the synthetic potential of this strategy.

Intramolecular Gold-Catalyzed Oxidation of Alkynes by Tethered Sulfoxides. The application of this concept was first realized using tethered sulfoxides as the oxygen-delivering oxidant by Toste³ and us⁴ independently at around the same time, and dihydrobenzothiepinones (e.g., 2) were formed in typically excellent yields (Scheme 2). Along the same line as in

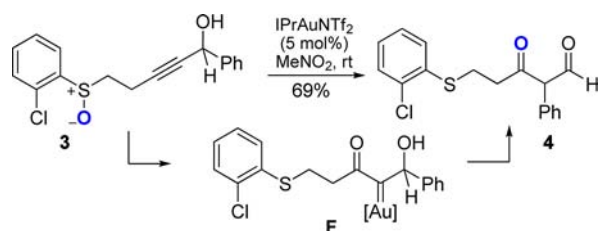
Received: April 28, 2012

Published: June 3, 2013

Scheme 2. Sulfoxides as Intramolecular Oxidants in Gold Catalysis^{3,4}

Scheme 1, a common mechanism via an α -oxo gold carbene intermediate (e.g., D) was proposed.^{3,4} In addition, we hypothesized the sulfonium ion E as a resting state of the gold carbene, although it might instead act to trap the gold carbene irreversibly. Particularly noteworthy in these reactions are the mild nature of sulfoxides as oxidants and the extremely high efficiencies in the formation of the seven-membered thiepinone ring. In an attempt to further explore its synthetic utility, we coupled the alkyne oxidation with a subsequent pinacol rearrangement upon modifying the phenyl group to hinder the benzothiepinone formation (Scheme 3), and β -diketones were

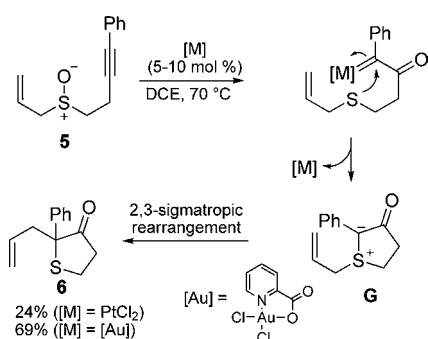
Scheme 3. Sequential Oxidation/Pinacol-Type Rearrangement



isolated in fair to good yields. The reaction results were consistent with the formation of a gold carbene intermediate F.

Later, Davies⁵ employed a similar strategy to access such a gold carbene (Scheme 4), which is subsequently trapped by the tethered nascent sulfide to form a sulfur ylide G. This intermediate, similar in nature to our previously proposed resting

Scheme 4. Tandem Gold-Catalyzed Intramolecular Alkyne Oxidation and 2,3-Sigmatropic Rearrangement via the Intermediacy of a Sulfur Ylide

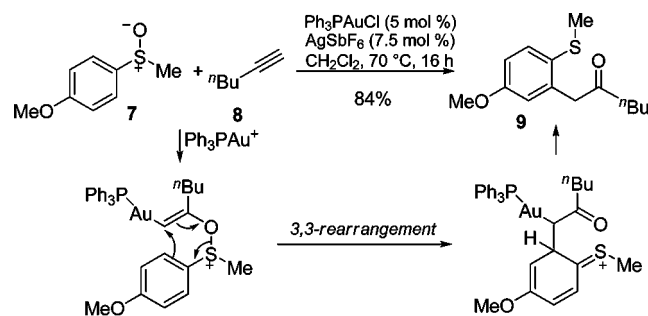


state E, underwent a [2,3]-sigmatropic rearrangement to render the final sulfur heterocycle. The fact that this mechanistic rationale is seemingly the only viable one for this transformation strongly suggests that α -oxo gold carbenes of type B are accessible via the strategy outlined in Scheme 1, but argues strongly that the sulfonium intermediate E should be formed in Scheme 2. This begs the question of why E, presumably much more stable than the gold carbene, does not impede the observed cyclization.

Many researchers including us have subsequently applied this intramolecular strategy to other oxygen-delivering oxidants including nitron,⁶ *N*-oxides,⁷ epoxide,⁸ and nitro⁹ successfully, under the assumption¹⁰ that α -oxo gold carbenes were generated.

Intermolecular Gold-Catalyzed Alkyne Oxidation Using Sulfoxides as Oxidants. With all these successes with intramolecular oxidations, intermolecular alkyne oxidation using sulfoxides was studied by Ujaque and Asensio.¹¹ However, in their elegant work, the experimental results do not support the formation of an α -oxo gold carbene intermediate of type B. Instead, a [3,3]-sigmatropic rearrangement is invoked to explain the reaction outcomes, which is further corroborated by computational studies (Scheme 5). This study prompted us to

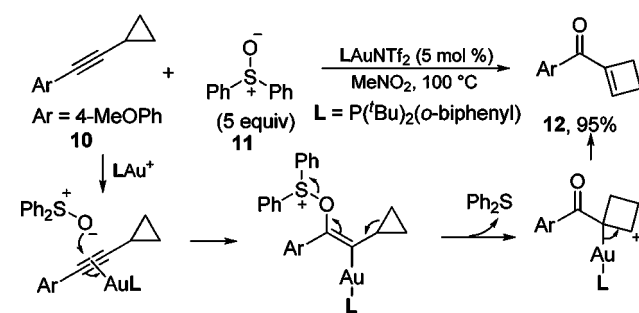
Scheme 5. Gold-Catalyzed Alkyne Oxidation by an External Sulfoxide



contemplate an alternative 3,3-rearrangement mechanism for the original intramolecular chemistry (see Scheme 2).^{3,4}

Later, Liu^{1k} reported a gold-catalyzed intermolecular oxidative ring expansion using Ph₂SO as the external oxidant. In the proposed mechanism (Scheme 6), no α -oxo gold carbene is

Scheme 6. Gold-Catalyzed Alkyne Oxidation by an External Sulfoxide



involved, and the reaction proceeds via a concerted ring expansion and ejection of nucleofugal Ph₂S.

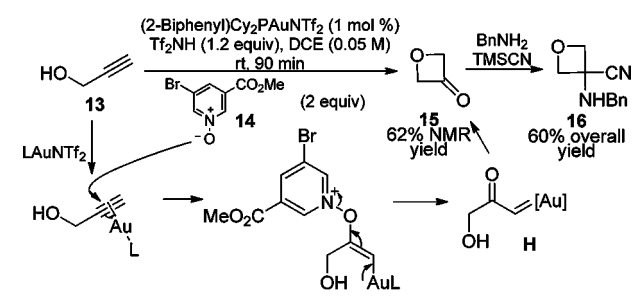
All these studies using sulfoxides as oxidants seemingly suggest that the reaction pathways depend simply on whether the oxidant is tethered or not, that is, [3,3]-rearrangement or concerted elimination when intermolecular and gold carbene

formation when intramolecular. This, however, need not be the case. Due to the tremendous synthetic potential of α -oxo gold carbenes, coupled with the surprisingly efficient formation of seven-membered thiepinone **2** and the absence of reaction inhibition due to the likely formation of sulfonium **E**, we embarked on mechanistic studies of the dihydrobenzothiepinone formation both experimentally and theoretically. Herein we disclose our findings and the extension of this chemistry to the formation of even larger S-heterocycles and to nonaromatic substrates.

RESULTS AND DISCUSSION

Mechanistic Studies of the Benzothiepinone Formation. In our continued effort to implement the general strategy shown in Scheme 1, we have recently reported the first case of successful generation of α -oxo gold carbenes using an external oxidant.¹² This strategy was later expanded by us to (1) an efficient synthesis of oxetan-3-ones from propargyl alcohols (Scheme 7),¹³ (2) a regioselective synthesis of α,β -unsaturated

Scheme 7. Generation of α -Oxo Gold Carbenes via Intermolecular Alkyne Oxidation and Its Application in Oxetan-3-one Formation



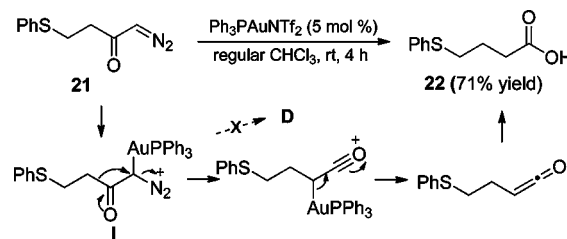
ketones from internal alkynes,¹⁴ (3) a rapid [2 + 2 + 1] approach to 2,5-disubstituted oxazoles,¹⁵ (4) a stereoselective synthesis of azetidin-3-ones from propargylic amides,¹⁶ and (5) a rapid access to chroman-3-ones.¹⁷ The suitable oxidants were not sulfoxides but pyridine *N*-oxides and quinoline *N*-oxides, and the formation of gold carbene intermediates (e.g., **H**) is strongly implicated in the formation of oxetan-3-ones (Scheme 7)¹³ and the azetidine-3-ones.¹⁶ To our delight, this strategy has also been adopted by other researchers in the development of versatile synthetic methods.¹⁸

This easy access to α -oxo gold carbenes from alkynes using external pyridine/quinoline *N*-oxides provided us a valuable opportunity to probe the mechanism of the dihydrobenzothiepinone formation. Hence, a variety of oxidants and gold catalysts were examined with alkynyl sulfide **17** as the substrate, but most of the reactions were messy, and none gave the

expected thiepinone **1**. Instead, α -chloroketone **19** was formed in <10% yields in some cases (e.g., Scheme 8), which was the result of chloride abstraction^{5a,19} from the reaction solvent, dichloroethane. This is consistent with the intermediacy of the highly electrophilic α -oxo gold carbene **D**. In addition, the rearranged enone **20** was formed during isolation, which can be explained via a cyclization and elimination process. As a control experiment, no sulfoxide was observed after stirring a mixture of sulfide **17** and the oxidant, 8-isopropylquinoline *N*-oxides **18**, in DCE for 20 h.

Pérez, Nolan, and Echavarren recently reported in several interesting studies²⁰ that gold catalysts could decompose α -diazooesters to access reactivities of gold carbenes such as C–H insertion and cyclopropanation. However, one experiment in our recent work¹⁰ led to our tentative conclusion that α -oxo gold carbenes might not be generated upon gold-catalyzed decomposition of α -diazoketones due to competing facile Wolff rearrangement. To exhaust all possible approaches to generating **D**, we nevertheless prepared α -diazoketone **21** and treated it with $\text{Ph}_3\text{PAuNTf}_2$ (5 mol %). No thiepinone **2** was detected and neither were the ketone products **19** and **20**. Instead, the carboxylic acid **22** was formed via apparent sequential Wolff rearrangement²² and hydration in a 71% isolated yield (Scheme 9).

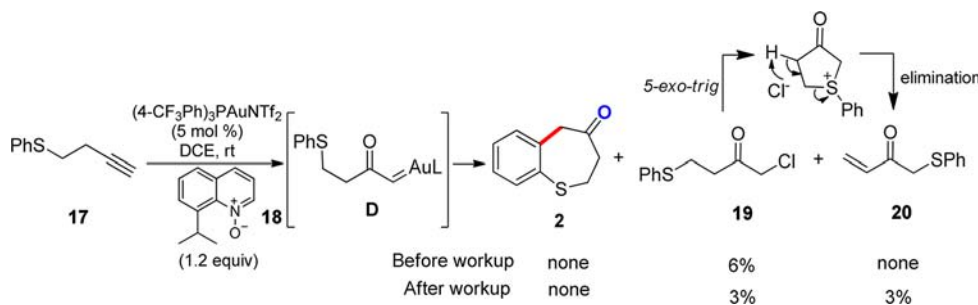
Scheme 9. Attempt To Generate Gold Carbene D via Dediazotization



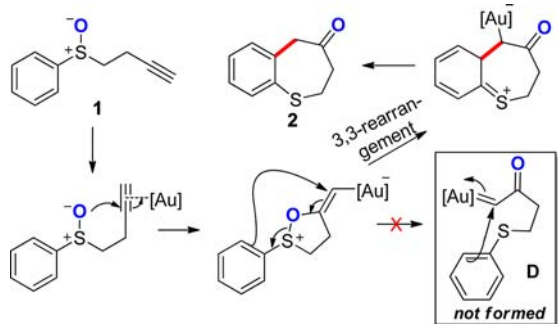
This result is consistent with our previous observation¹⁰ and likewise suggests that the gold carbenoid **I** instead of the gold carbene **D** is most likely the reactive intermediate generated. It is worthwhile to point out that the mechanism of the Wolff rearrangement catalyzed by metal complexes including preferred silver salts has not been clearly elucidated.

These results raise serious doubts about the nature of the gold intermediate en route to the thiepinone **2**. If one of the reaction intermediates were indeed the gold carbene **D**, it might then be expected to abstract chloride, as in Scheme 8, and/or be trapped as the sulfonium species **E**. An alternative mechanism, in line with the intermolecular studies,¹¹ would be a [3,3]-rearrangement for the key C–C bond forming step (Scheme 10). This would also readily explain the facile formation of seven-membered thiepinones and the absence of catalyst trapping by **E**.

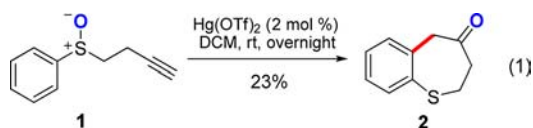
Scheme 8. Access to Gold Carbene D via Intermolecular Oxidation



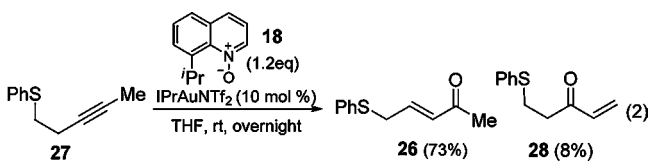
Scheme 10. Alternative Mechanism for Benzothiepinone Formation



The revised mechanism suggests that other metals could catalyze this cycloisomerization as long as they could promote the initial *S*-*exo*-*dig* cyclization. Indeed, $\text{Hg}(\text{OTf})_2$ promotes this reaction, albeit in a much lower efficiency (eq 1).

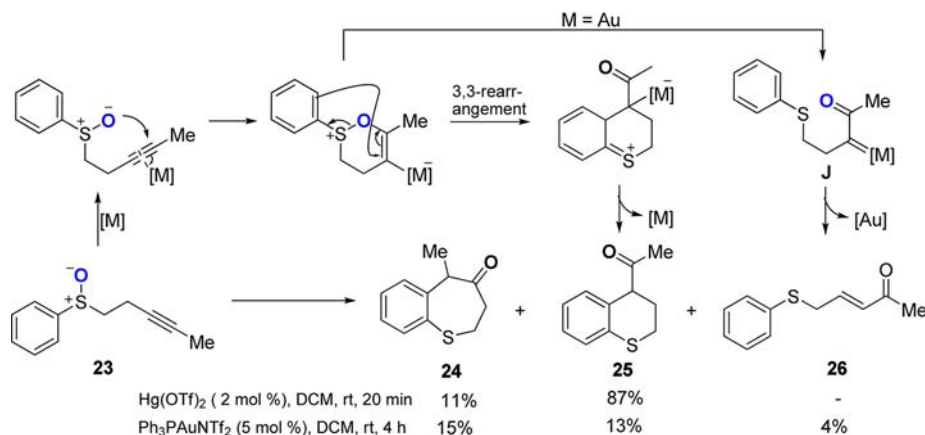


In the case of the sulfoxide **23** containing an internal alkyne (Scheme 11), $\text{Hg}(\text{OTf})_2$ catalyzed the cycloisomerization with a much higher overall efficiency. Besides the formation of the methylated thiepinone **24** as the minor product, the formation of the major product, the thiochroman **25**, could also be explained by a [3,3]-rearrangement, which is preceded by a likely favored 6-*endo*-*dig* cyclization. When $\text{Ph}_3\text{PAuNTf}_2$ was used as the catalyst, a small amount of the enone **26** was detected, indicative of competing formation of carbene intermediate **J**. The thiochroman **25** could be also formed from **J** via a Friedel–Crafts-type cyclization; however, this alternative was not supported by an intermolecular study. As shown in eq 2, following the intermolecular oxidation protocol¹⁴



we previously developed, the enone **26** was formed as the major regioisomer in a good yield; notably, neither **24** nor **25** was detected.

Scheme 11. Gold-Catalyzed Oxidation of Internal Alkyne by a Tethered Sulfoxide

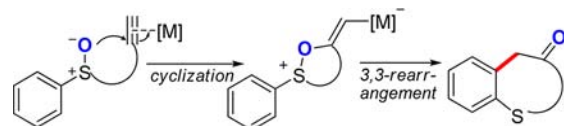


As the gold carbene **J** was most likely the formed intermediate en route to **26**, this result suggests that the apparent carbene 1,2-*C*-*H* insertion handily outcompetes cyclization, which in turn corroborates that **25** was formed via a [3,3]-rearrangement.

Formation of Benzene-Fused Larger S-Heterocycles.

With a better understanding of the reaction mechanism, we reasoned that benzene-fused larger S-heterocycles could be readily accessible via metal-catalyzed cycloisomerizations, provided that the initial sulfoxide cyclization could be realized (Scheme 12).

Scheme 12. Synthesis of Benzene-Fused Larger S-Heterocycles



In our early work,²³ the cycloisomerization of sulfoxide **29a** was examined only with dichloro(2-picolinato)gold(III) (Table 1, entry 1) under the assumption that the formation

Table 1. Catalyst Screening for the Formation of **30a**

entry	catalyst	time	yield ^a (%)
1	dichloro(2-picolinato)gold(III)	12 h	52 ^b
2	$\text{Ph}_3\text{PAuNTf}_2$	4 h	97
3	IPrAuNTf_2	4 h	74 ^c
4	$(4\text{-CF}_3\text{Ph})_3\text{PAuNTf}_2$	4 h	82
5	$\text{Hg}(\text{OTf})_2$	40 min	75 ^d

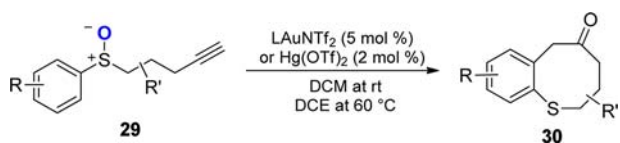
^aNMR yield using diethyl phthalate as reference. ^bData from our previous paper; ^cthe reaction was run at 50 °C. ^d20% of **29a** left. ^eMethyl ketone (20%) was formed due to alkyne hydration.

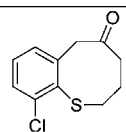
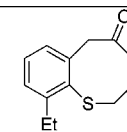
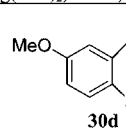
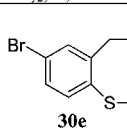
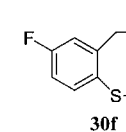
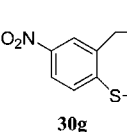
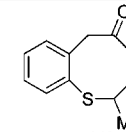
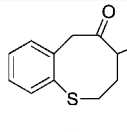
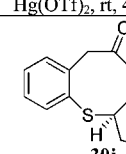
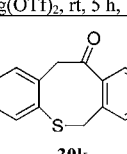
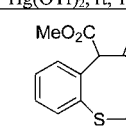
of a thiochroman ring via gold carbene cyclization would be too challenging. Indeed, the reaction yield was modest. However, a quick screening of gold catalysts revealed that the common gold catalyst, $\text{Ph}_3\text{PAuNTf}_2$,²¹ was highly effective, and dihydrobenzothiepinone **30a** was formed in 97% yield (entry 2),

consistent with the [3,3]-rearrangement mechanism. Other gold catalysts were capable of catalyzing this reaction, as well, albeit with lower efficiencies (entries 3 and 4). Hg(OTf)₂ again was effective, although a competing hydration was observed, and the reaction was much faster than in the cases of gold catalysis (entry 5).

To probe the reaction scope, the benzene ring of **29a** was substituted with groups of varying electronic natures at either the *ortho* or the *para* position. All the cases studied (Table 2,

Table 2. Scope Studies of Benzothiocinone Formation^a



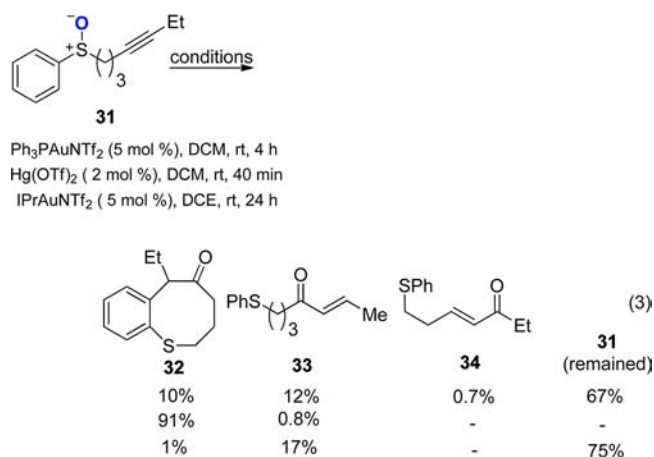
1	2
	
30b Ph ₃ PAuNTf ₂ , 60 °C, 24 h, 47% (42% ^b) Hg(OTf) ₂ , DCM, rt, 3 h, 96%	30c IPrAuNTf ₂ , 60 °C, 3 h, 97% Hg(OTf) ₂ , rt, 40 min, 84%
3	4
	
30d IPrAuNTf ₂ , 60 °C, 3 h, 61% Hg(OTf) ₂ , rt, 40 m, 72%	30e IPrAuNTf ₂ , 60 °C, 17 h, 29%(65% ^b) Hg(OTf) ₂ , rt, 2 h, 90%
5	6
	
30f IPrAuNTf ₂ , 60 °C, 17 h, 44%(50% ^b) Hg(OTf) ₂ , rt, 1.5 h, 76%	30g IPrAuNTf ₂ , 60 °C, 17 h, 10%(90% ^b) Hg(OTf) ₂ , rt, 12 h, 78%
7	8
	
30h IPrAuNTf ₂ , 60 °C, 6 h, 82% Hg(OTf) ₂ , rt, 4 h, 42%	30i Ph ₃ PAuNTf ₂ , rt, 23 h, 54%(30% ^b) Hg(OTf) ₂ , rt, 5 h, 77%
9	10
	
30j IPrAuNTf ₂ , 60 °C, 14 h, 87% Hg(OTf) ₂ , rt, 14 h, 76%	30k IPrAuNTf ₂ , 60 °C, 12 h, trace Hg(OTf) ₂ , rt, 22 h, 53%
11	
	
30m Ph ₃ PAuNTf ₂ , rt, 24 h, 75% Hg(OTf) ₂ , rt, 24 h, 42%	

^a[**29**] = 0.05 M. Isolated yield reported. ^bUnreacted substrate.

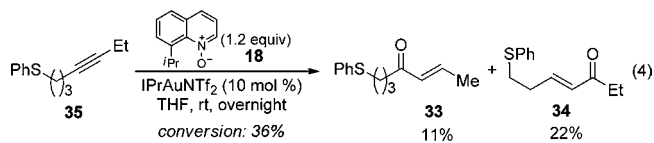
entries 1–6) worked smoothly and efficiently with Hg(OTf)₂ as the catalyst. IPrAuNTf₂ was found to be the best gold catalyst in most cases but was generally less efficient than Hg(OTf)₂. Moreover, Au catalysis was much slower than that by Hg(OTf)₂ in these cases. Aliphatic substitutions at the pentynyl chain were allowed (entries 7–9). Interestingly, the positions of their

attachment strongly influenced the reaction outcomes for both Au and Hg but with opposite trends: with a 5-methyl group, IPrAuNTf₂ was the better catalyst; with a *n*-butyl group at the 3-position, Hg(OTf)₂ was better. *cis*-Fusion of the pentynyl chain with a cyclohexane ring at the 4,5-positions caused no problem for the chemistry (entry 9), but a 3,4-fusion with a benzene ring only permitted the Hg catalysis in a moderate yield (entry 10). The sulfoxide **29m** containing an electron-deficient C–C triple bond was allowed (entry 11), and in this case, IPrAuNTf₂ was better.

When sulfoxide **31** containing an ethyl group at the alkyne terminus was treated with Ph₃PAuNTf₂, both the cyclized product **32** and the enone **33** derived from an initial 6-*exo-dig* cyclization were formed (eq 3); in addition, the enone **34**

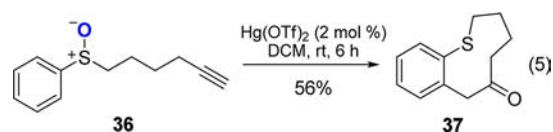


formed from an initial 7-*endo-dig* cyclization was detected as trace material. Somewhat to our surprise, Hg(OTf)₂ promoted the formation of **32** rapidly and efficiently, with only a trace amount of **33** formed. The Hg counterpart²⁴ of α -oxo gold carbene **B** may be difficult to form. These results point to divergent mechanisms, similar to those shown in Scheme 11, where **32** is formed via a [3,3]-rearrangement of the initial 6-*exo-dig* cyclization intermediate, and **33** is formed via an α -oxo gold carbene intermediate. Indeed, no cyclized product was observed when the sulfide **34** was subjected to intermolecular oxidation by 8-methylquinoline *N*-oxide, confirming that the thiocinone **32** was not formed via a gold carbene intermediate (eq 4). Notably, when IPrAuNTf₂ was used as the



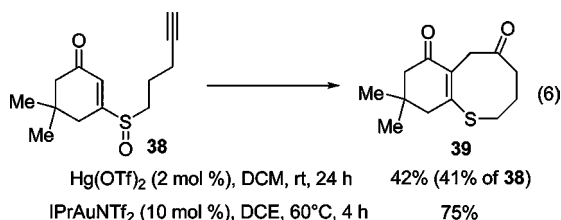
catalyst, **33** was formed at the expense of **32** (see Eq 3), which nevertheless is consistent with the fact that IPr is a much better σ -donor than Ph₃P and hence can facilitate the formation of electrophilic gold carbene intermediates, thereby favoring the enone formation.

Even a nine-membered S-heterocycle could be readily prepared via this cycloisomerization approach (eq 5). Hg(OTf)₂

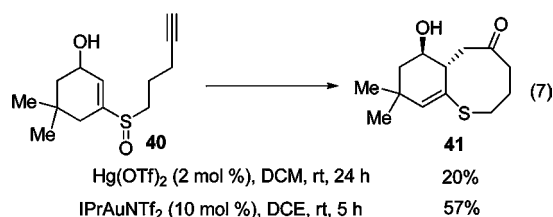


turned out to be the catalyst of choice, and various gold complexes did not promote this reaction.

With the aromatic ring merely providing a C–C double bond in the [3,3]-rearrangement, we reason that a simple C–C double bond would play a similar, if not a better, role. Indeed, when enone sulfoxide **38** was treated with IPrAuNTf_2 , cyclohexenone-fused dihydrothiicinone **39** was formed in 75% yield. A lower yield was observed with $\text{Hg}(\text{OTf})_2$ as the catalyst (eq 6). In addition, the enone could be reduced into the allylic alcohol



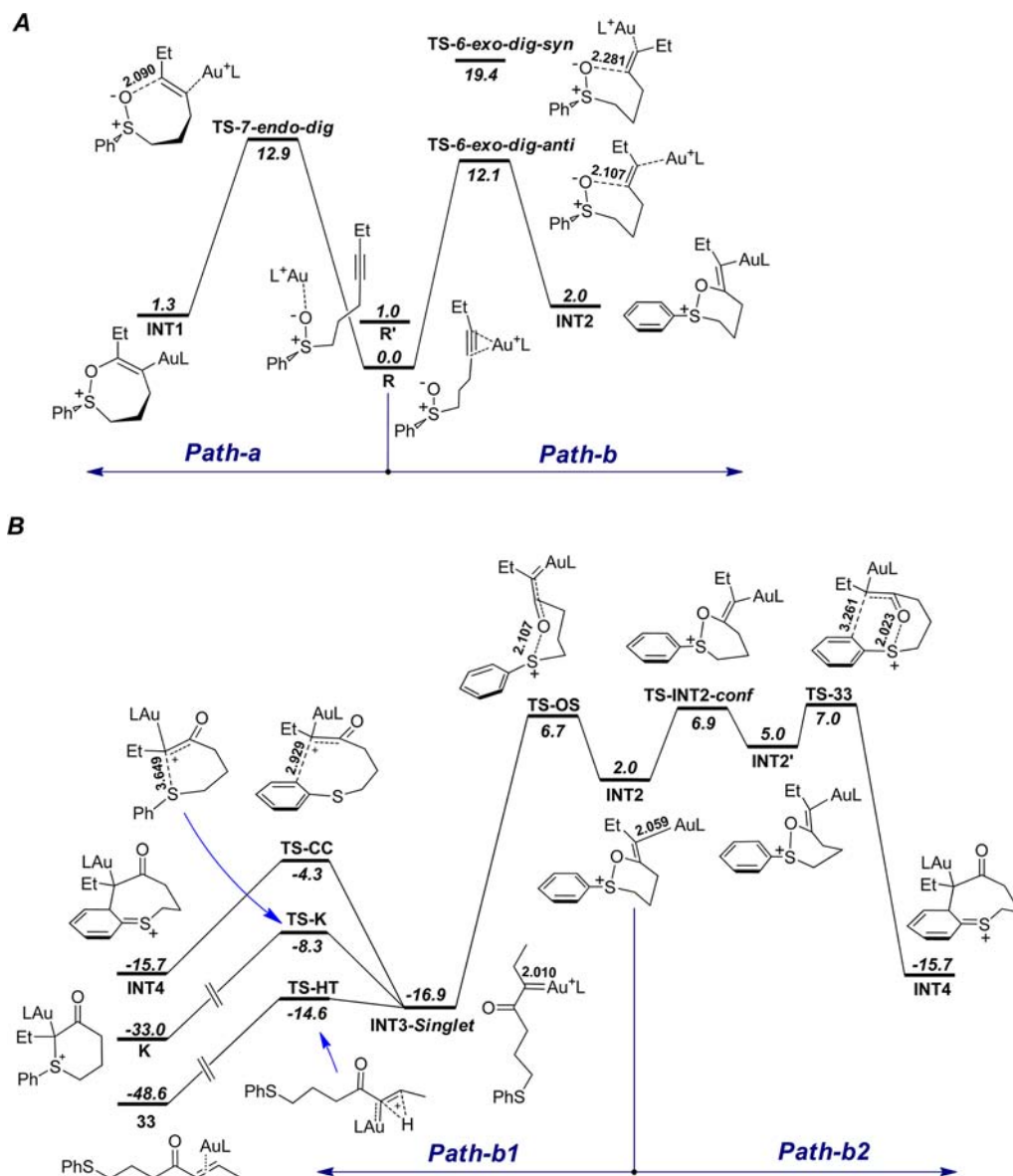
40. To our delight, it underwent a similar cyclization and [3,3]-rearrangement process albeit with decreased efficiency in the case of either a Au catalyst or $\text{Hg}(\text{OTf})_2$, affording the product **41** with the double bond migrated (eq 7).



■ COMPUTATIONAL STUDIES

To provide theoretical support for the [3,3]-sigmatropic rearrangement mechanism, density functional theory (DFT)²⁵ studies have been

Scheme 13. Calculated Reaction Pathways for Substrate **31**^a



^a(A) (*Path-a*) 7-endo-dig and (*Path-b*) 6-exo-dig cyclization of the reactant complex **R**. (B) Gold carbene intermediate pathway (*Path-b1*) and the [3,3]-sigmatropic rearrangement pathway (*Path-b2*) of the alkenylgold intermediate **INT2**. The selected bond lengths are in angstroms, and the relative free energies in dichloromethane ($\Delta G_{\text{sol}}^{\circ}$) are in kcal/mol. Calculated at the PBE1PBE/6-31+G**/SDD level.

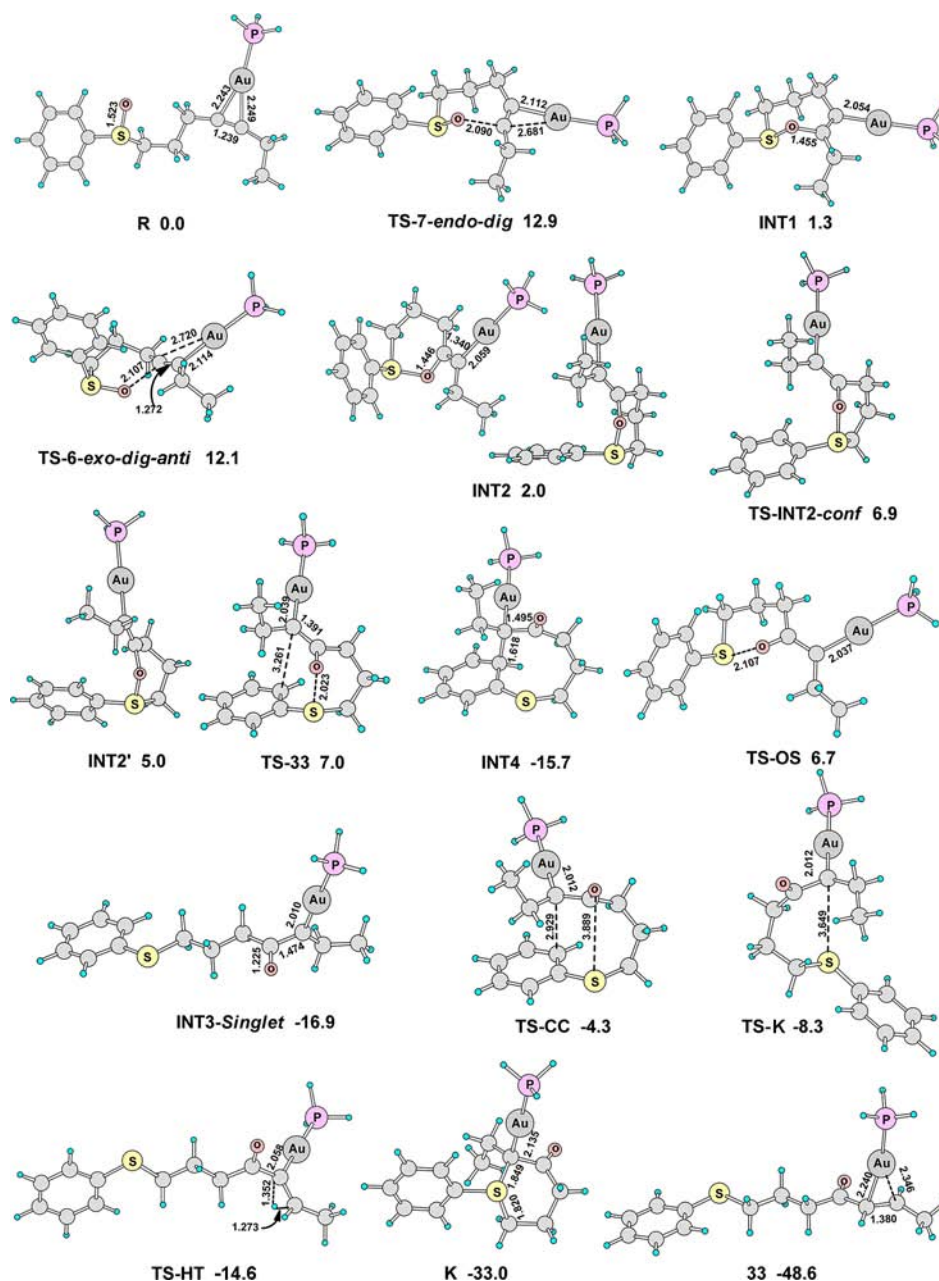


Figure 1. Main optimized structures on the reaction pathways shown in Scheme 13. The selected bond lengths are in angstroms, and the relative free energies in dichloromethane ($\Delta C_{\text{sol}}^{\circ}$) are in kcal/mol. Calculated at the PBE1PBE/6-31+G**/SDD level.

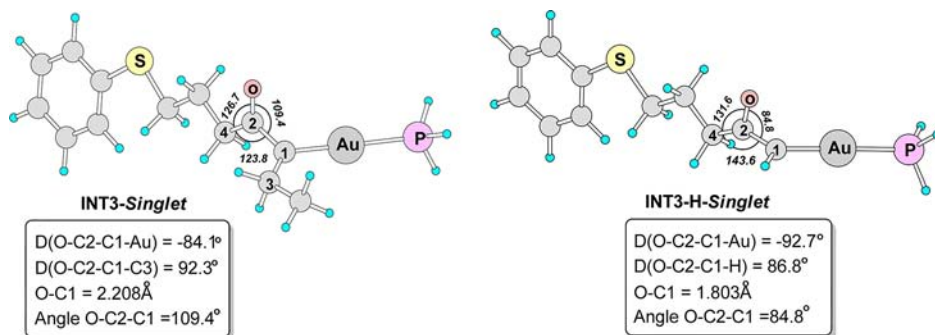


Figure 2. Optimized singlet states of α -oxo gold carbene structures with terminal ethyl (INT3-singlet) and H group (INT3-H-singlet). The selected bond lengths are in angstroms, angles are in degrees. Calculated in dichloromethane at the PBE1PBE/6-31+G**/SDD level.

performed with the GAUSSIAN09 program²⁶ using the PBE1PBE²⁷ method. For C, H, O, N, P, and S, the 6-31+G** basis set was

used, and for Au and Hg, the SDD basis set with an effective core potential (ECP)²⁸ was used. Geometry optimization was performed in

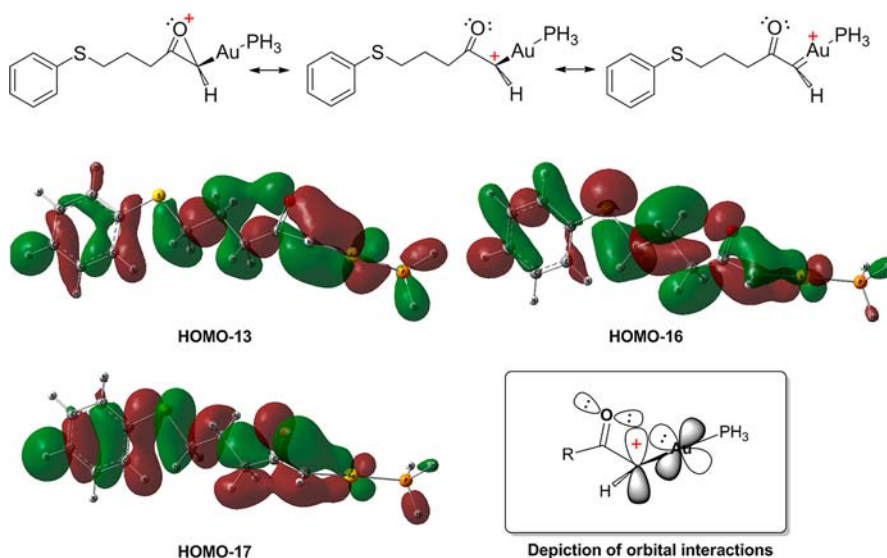
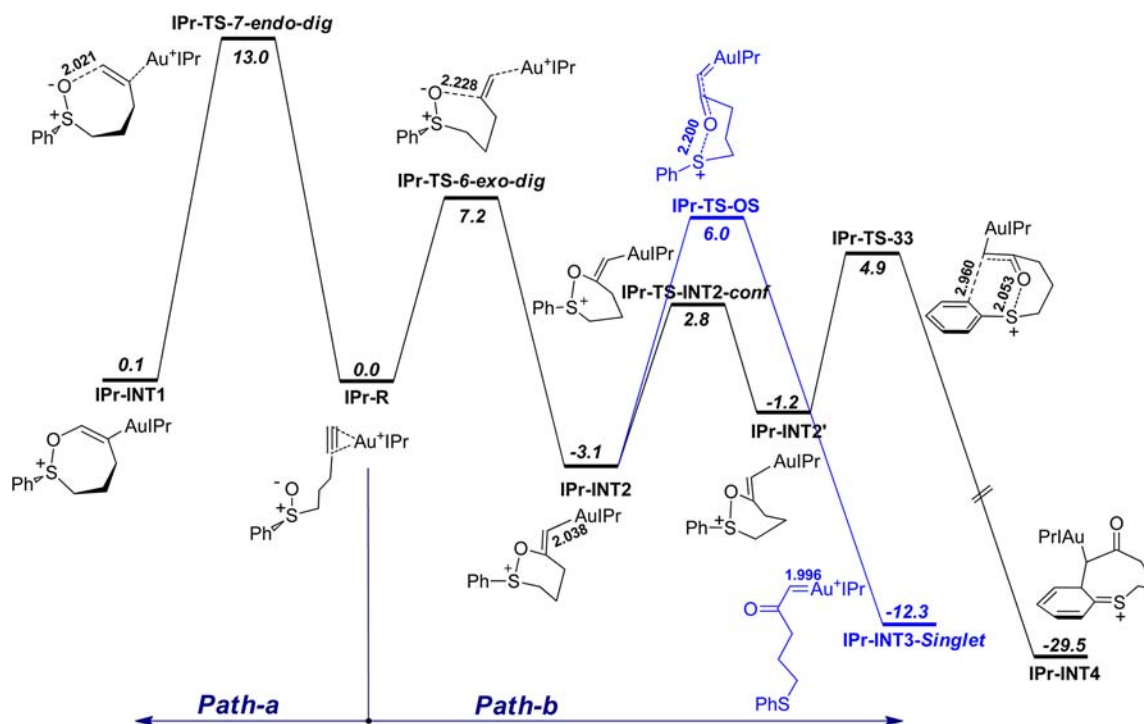


Figure 3. Selected molecular orbitals and the depiction of the orbital interactions in the singlet state α -oxo gold carbene INT3-H-singlet.

Scheme 14. Calculated Reaction Pathways of the Substrate 29a^a



^aThe selected bond lengths are in angstroms, and the relative free energies in dichloromethane ($\Delta G_{\text{sol}}^{\circ}$) are in kcal/mol. Calculated at the PBE1PBE/6-31+G**/SDD level.

dichloromethane using the SMD²⁹ method. Harmonic vibration frequency calculations were carried out, and the optimized structures are all shown to be either minima (with no imaginary frequency) or transition states (with one imaginary frequency). Reactions with three different substrates were calculated. First, the reaction shown in eq 3 was explored by using the simplified H_3P as the metal ligand. The likely competing occurrence of the gold carbene pathway and the [3,3]-sigmatropic rearrangement pathway in this reaction makes it an excellent case for theoretical studies. Then, the sulfoxide 29a, which differs from 31 by having a terminal alkyne, was examined using the experimentally employed catalyst IPrAu^+ . Finally, the reaction of the homopropargyl sulfoxide 1 (Scheme 2), reported by both Toste³ and us⁴ in the pioneer studies of gold carbene chemistry, was studied. All the calculations

support the experimental conclusion that the cyclized products are formed via the [3,3]-sigmatropic rearrangement pathway, where no gold carbene intermediate is involved.

Reaction Pathways of the Sulfoxide 31. As shown in Scheme 13, the complex of 31 and H_3PAu^+ , R, may undergo 7-endo-dig (TS-7-endo-dig, $\Delta G_{\text{sol}}^{\circ} = 12.9$ kcal/mol) or 6-exo-dig-anti (TS-6-exo-dig, $\Delta G_{\text{sol}}^{\circ} = 12.1$ kcal/mol) cyclization to afford the intermediates INT1 or INT2, respectively. The 6-exo-dig cyclization (Path b) is slightly more favorable (with full models, the energy difference increases to 1.3 kcal/mol),³⁰ qualitatively consistent with the experimental observations that the products resulting from the 6-exo-dig cyclization (i.e., 32 and 33, eq 3) were dominant. Another reactant complex R', in which the gold coordinates with the sulfoxide oxygen,

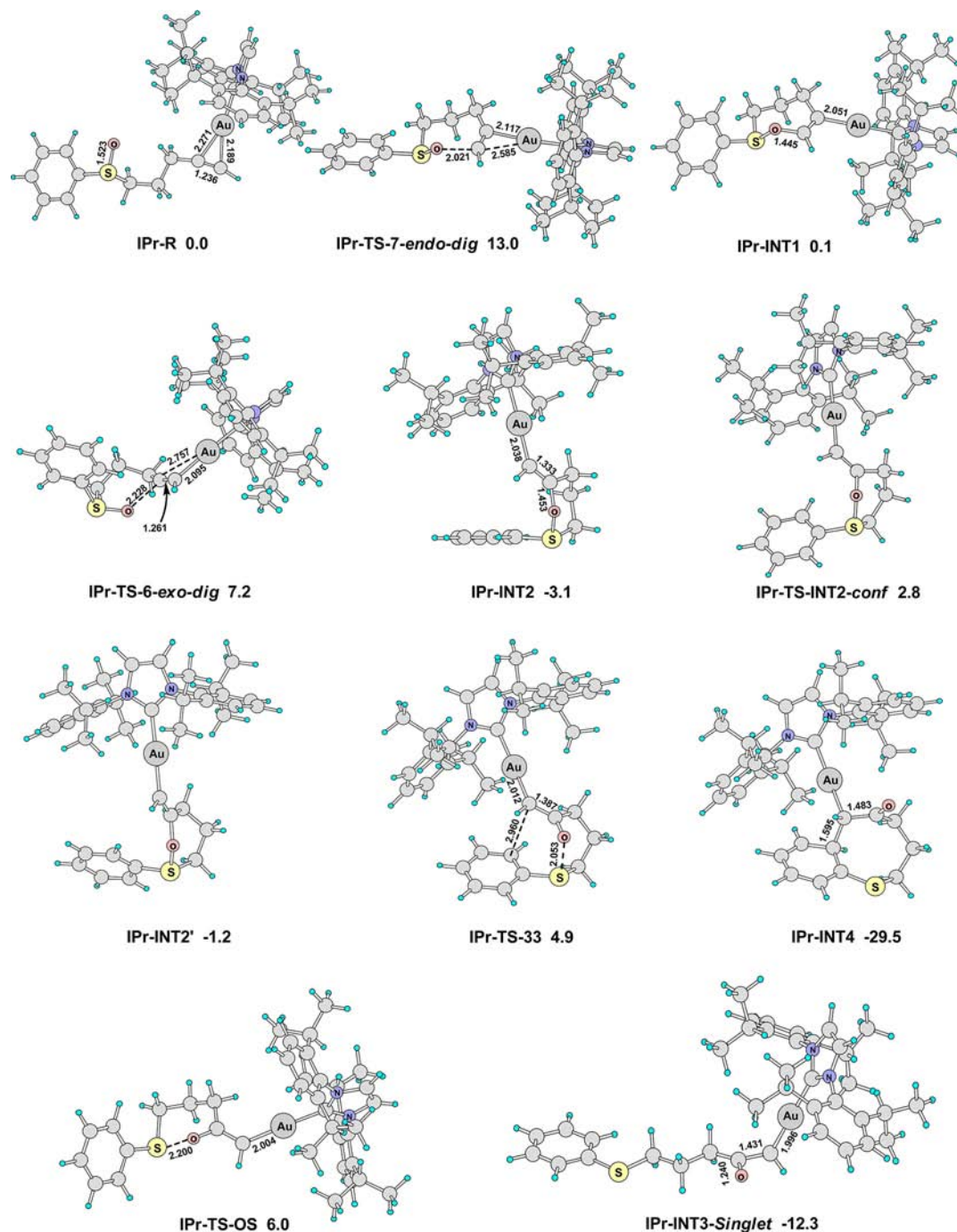


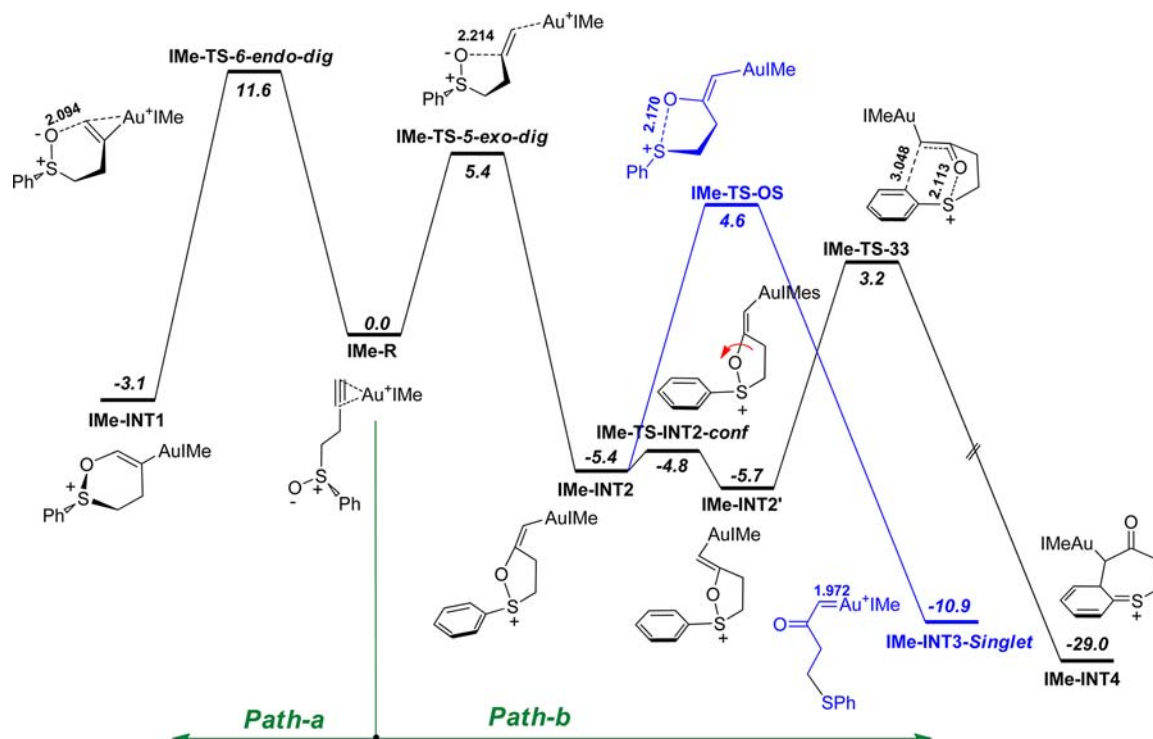
Figure 4. Main optimized structures on the reaction pathways shown in Scheme 14. The selected bond lengths are in angstroms, and the relative free energies in dichloromethane ($\Delta G_{\text{sol}}^{\circ}$) are in kcal/mol. Calculated at the PBE1PBE/6-31+G**/SDD level.

is 1.0 kcal/mol less stable than **R**, and its *syn* addition to the tethered alkyne (**TS-6-*exo-dig-syn***) has an energy barrier of 19.4 kcal/mol, much higher than that of **TS-6-*exo-dig-anti*** (Figure 1).¹⁰

There are two likely pathways for the alkenylgold intermediate **INT2** to proceed. One is *Path-b1*, where it undergoes S–O bond breaking (**TS-OS**) to afford the α -oxo gold carbene intermediate, of which the singlet state is the ground state (**INT3-singlet**).³⁰ The C–Au bond length in **INT2** is 2.059 Å, which is decreased to 2.010 Å in **INT3-singlet**, indicating a significant interaction between the carbocation and the Au atom, which can be ascribed to the π -donation of the 5d electrons of the Au atom.³¹ The NBO³² charge on Au is increased from +0.220 in **INT2** to +0.371 in **INT3-singlet**.

As shown in Figure 2, interestingly, in **INT3-singlet**, the carbonyl group (C2–O) is nearly perpendicular to the C3–C1–Au plane.

The angle O–C2–C1 is 109.4°, smaller than the other two angles O–C2–C4 (126.7°) and C1–C2–C4 (123.8°), showing that the carbonyl oxygen atom becomes closer to C1. The calculated Wiberg bond index³³ of O–C1 is 0.2112, indicating that, to some extent, the lone pair of the carbonyl oxygen atom fills the empty p orbital on C1, stabilizing the carbocation. These features are much more pronounced in **INT3-H-singlet**: the angle O–C2–C1 decreases dramatically to 84.8°, and the O–C1 distance decreases to 1.803 Å, and the calculated Wiberg bond index of O–C1 increases to 0.6154. Without the electron-donating ethyl group, the carbonyl oxygen atom has a very strong interaction with C1. The structure of the α -oxo gold carbene intermediate may be rationalized by the resonance structures shown in Figure 3. The interaction between the lone pair of the carbonyl oxygen atom and the empty p orbital of the carbocation is supported by the

Scheme 15. Calculated Reaction Pathways for Substrate 1^a

^aThe selected bond lengths are in angstroms, and the relative free energies in dichloromethane ($\Delta G_{\text{sol}}^{\circ}$) are in kcal/mol. Calculated at the PBE1PBE/6-31+G**/SDD level.

molecular orbital analysis. In the α -oxo gold carbene, in addition to the π -donation of the 5d electrons of the Au atom, the lone pair of the carbonyl oxygen atom is also involved in the stabilization of the carbocation.

For the gold carbene intermediate INT3-singlet, the 1,2-H shift (TS-HT) is very easy, with only a small energy barrier of 2.3 kcal/mol to form the enone product 33. In contrast, the energy barrier for the Friedel–Crafts-type electrophilic aromatic substitution reaction via TS-CC is much higher (12.6 kcal/mol). The trapping of the gold carbene by the tethered sulfide to form of the sulfonium ion K has a barrier of intermediate energy of 8.6 kcal/mol. These results indicate that the benzothiocinone 32 cannot be obtained from the gold carbene intermediates since the Friedel–Crafts pathway leading to its formation is much less favorable than the 1,2-H shift. The 1,2-H shift, hence, is the predominant route for the decomposition of the gold carbene intermediate, consistent with the experimental observation (eq 3). Even for substrates where the 1,2-H shift pathway is not available, the formation of sulfoniums of type E (see Scheme 2) could be substantially favored over the Friedel–Crafts-type cyclization.

Alternatively, after a conformational conversion (TS-INT2-conf), INT2' may undergo a [3,3]-sigmatropic rearrangement (TS-33) to afford INT4, which will lead to the benzothiocinone product 32 after 1,2-H shift.³⁰ The lengths of the breaking O–S bond and the forming C–C bond are 2.023 and 3.261 Å, respectively, comparable to that of the former theoretical study (2.565 and 3.251 Å).¹¹

The barriers of the competing product-forming steps from INT2 are close to each other for Path-b1 (TS-OS, $\Delta G_{\text{sol}}^{\circ}$ = 6.7 kcal/mol) and Path-b2 (TS-33, $\Delta G_{\text{sol}}^{\circ}$ = 7.0 kcal/mol), which is consistent with the formation of both 32 and 33 experimentally. With full models, the energy difference between TS-OS and TS-33 is 0.2 kcal/mol.³⁰

When using Hg(OTf)₂ as the catalyst, Hg cannot stabilize the carbocation like Au does due to a much weaker relativistic effect,³⁴ thus the energy of the S–O bond breaking transition state will increase relative to that of the [3,3]-sigmatropic rearrangement. The calculations show that Hg-TS-33 is much more favorable than Hg-TS-OS,³⁰ thus the cyclic product 32 was obtained predominantly.

As we were preparing this paper, DFT studies³⁵ of the gold-catalyzed rearrangements of alkynyl aryl sulfoxides appeared. Notably, only the reaction pathways involving the generation of gold carbene intermediates and their subsequent Friedel–Crafts cyclizations, identical to the original proposed mechanisms by Toste³ and us,⁴ were calculated. The [3,3]-sigmatropic rearrangement pathway and the gold carbene pathways involving the 1,2-hydride migration and the formation of sulfonium species were not considered. Although the Friedel–Crafts cyclizations by gold carbene moieties have calculated energy barriers ranging from 6.0 to 22.8 kcal/mol, they are, as we have shown both experimentally and by calculation, not likely to be the processes leading to the cyclized product.

Reaction Pathways of Sulfoxide 29a. Based on the systematic theoretical studies with the sulfoxide 31, similar reaction pathways were also obtained with the sulfoxide 29a, which instead is a terminal alkyne. To reflect the fact that IPrAuNTf₂ was also an effective catalyst (Table 1), the calculation used the full model of IPr as the metal ligand³⁶ (Scheme 14 and Figure 4).

As shown in Scheme 14, the 6-exo-dig cyclization (IPr-TS-6-exo-dig) is much favorable than 7-endo-dig cyclization (IPr-TS-7-endo-dig) by 5.8 kcal/mol, which is consistent with the experimental observations that only the product resulting from the 6-exo-dig cyclization (i.e., 30a) was observed. In the competing product-forming steps from IPr-INT2, the barrier of [3,3]-sigmatropic rearrangement (IPr-TS-33, $\Delta G_{\text{sol}}^{\circ}$ = 4.9 kcal/mol) is lower than that of O–S bond breaking (IPr-TS-OS, $\Delta G_{\text{sol}}^{\circ}$ = 6.0 kcal/mol), which is consistent with the formation of 30a experimentally. The α -oxo gold carbene intermediate IPr-INT3-singlet has structural features similar to that of INT3-H-singlet (Figure 2).

The preference to the [3,3]-sigmatropic rearrangement pathway by the sulfoxide 29a, in relation to the case of 31, can be qualitatively rationalized: when the electron-donating ethyl group of 31 is changed to the hydrogen in 29a, the stabilization of the corresponding transition state TS-OS by the ethyl group is lost, whereas during the [3,3]-sigmatropic rearrangement the steric congestion caused by the ethyl group in TS-33 is relieved, and the electrophilicity of the carbon center *ipso* to AuL in IPr-TS-33 should increase. All the factors should

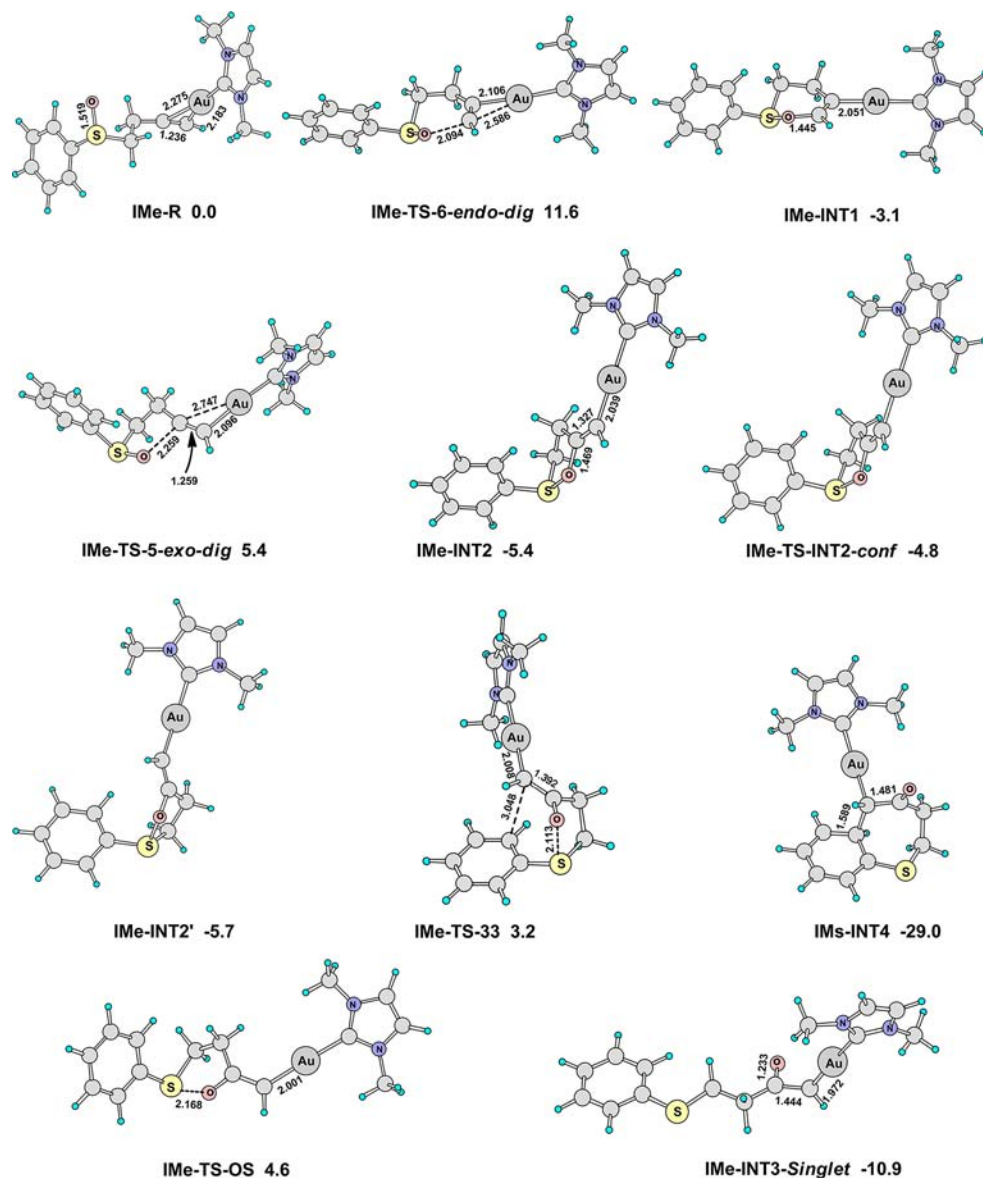


Figure 5. Main optimized structures on the reaction pathways shown in Scheme 15. The selected bond lengths are in angstroms, and the relative free energies in dichloromethane ($\Delta G_{\text{sol}}^{\circ}$) are in kcal/mol. Calculated at the PBE1PBE/6-31+G**/SDD level.

synergistically promote the benzothioinone formation relative to the gold carbene pathway.

Reaction Pathways of Sulfoxide 1. As discussed in the Introduction, the gold-catalyzed transformation of **1** is a pioneer reaction in gold carbene chemistry. While the experimental studies suggest strongly that gold carbene intermediates are not involved in the formation of benzothiepinones, DFT calculations of the reaction would provide further support for the conclusion. As shown in Scheme 15 and Figure 5, the calculated reaction pathways using IMe as the metal ligand are similar to that of **29a**. The 5-*exo-dig* cyclization (IMe-TS-5-*exo-dig*) is favorable than 6-*endo-dig* cyclization (IMe-TS-6-*endo-dig*) by 6.2 kcal/mol, and the barrier of [3,3]-sigmatropic rearrangement (IMe-TS-33, $\Delta G_{\text{sol}}^{\circ} = 3.2$ kcal/mol) is more favorable than that of O–S bond breaking (IMe-TS-OS, $\Delta G_{\text{sol}}^{\circ} = 4.6$ kcal/mol).

CONCLUSION

Through a combination of experiments and density functional theory studies, we have addressed lingering questions on the mechanism of gold-catalyzed intramolecular oxidation of terminal alkynes with an arenesulfinyl group as the tethered oxidant. The previous proposed mechanism for the formation

of benzothiepinone via Friedel–Crafts-type cyclizations of α -oxo gold carbene intermediates is disproved experimentally by generating these reactive species via intermolecular oxidation and by extensive DFT studies, which reveal a high energy barrier for such cyclizations relative to a 1,2-H shift or an intramolecular trapping by the tethered nascent sulfide. Instead, a [3,3]-sigmatropic rearrangement of the initial cyclization intermediate offers a reaction path that is consistent with both experimental results and the theoretical data. With internal alkyne substrates, however, the intermediacy of a gold carbene species becomes possible. This reactive intermediate, nevertheless, does not proceed to afford the Friedel–Crafts-type cyclization product. Instead, a facile 1,2-H shift leads to exclusive formation of an enone product. The [3,3]-sigmatropic rearrangement can still compete with gold carbene formation, yielding mid-sized sulfur-containing cycloalkenone products. With this new mechanistic insight, the product scope of this versatile formation of mid-sized sulfur-containing cycloalkenones has been expanded to various dihydrobenzothioinones and even a tetrahydrobenzocyclononone. Besides

benzenesulfinyl substrates, alkynes with a tethered alkenylsulfinyl group can likewise participate in the [3,3]-sigmatropic rearrangement, leading to mid-sized S-heterocycles without the entanglement of the fused benzene ring. This opens a new opportunity for accessing a diverse range of substituted mid-sized S-heterocycles. Besides gold, Hg(OTf)₂ can be an effective catalyst, thereby offering a cheap alternative for this intramolecular redox reaction.

■ ASSOCIATED CONTENT

Supporting Information

Experimental procedures, compound characterization and spectra, all the structures in the calculated pathways, the relaxed potential energy surface (PES) scan, and the calculated total energies and geometrical coordinates. This material is available free of charge via the Internet at <http://pubs.acs.org>.

■ AUTHOR INFORMATION

Corresponding Author

zhang@chem.ucsb.edu; liyuxue@sioc.ac.cn

Present Addresses

#Shanghai Hengrui Pharmaceuticals Co. Ltd, Shanghai, 200245, P. R. China

Notes

The authors declare no competing financial interest.

■ ACKNOWLEDGMENTS

B.L., Y.L., and L.Z. thank NSF (CAREER CHE-0969157) and NIGMS (R01 GM084254) for generous financial support. L.Z. thanks PIRE-ECCI for supporting the collaboration between him and Y.L. Y.L. thanks the National Natural Science Foundation of China (Grant Nos. 21172248, 21121062). D.A. acknowledges support from the Center for Scientific Computing at the CNSI and MRL (NSF MRSEC DMR-1121053 and NSF CNS-0960316) and the National Center for Supercomputing Applications (NSF TG-CHE100123) utilizing the NCSA Gordon and Blacklight systems.

■ REFERENCES

- (1) (a) Fürstner, A.; Davies, P. W. *Angew. Chem., Int. Ed.* **2007**, *46*, 3410–3449. (b) Hashmi, A. S. K. *Chem. Rev.* **2007**, *107*, 3180–3211. (c) Ma, S.; Yu, S.; Gu, Z. *Angew. Chem., Int. Ed.* **2006**, *45*, 200–203. (d) Zhang, L.; Sun, J.; Kozmin, S. A. *Adv. Synth. Catal.* **2006**, *348*, 2271–2296. (e) Arcadi, A. *Chem. Rev.* **2008**, *108*, 3266–3325. (f) Jiménez-Núñez, E.; Echavarren, A. M. *Chem. Rev.* **2008**, *108*, 3326–3350. (g) Li, Z.; Brouwer, C.; He, C. *Chem. Rev.* **2008**, *108*, 3239–3265. (h) Patil, N. T.; Yamamoto, Y. *Chem. Rev.* **2008**, *108*, 3395–3442. (i) Gorin, D. J.; Sherry, B. D.; Toste, F. D. *Chem. Rev.* **2008**, *108*, 3351–3378. (j) Abu Sohel, S. M.; Liu, R.-S. *Chem. Soc. Rev.* **2009**, *38*, 2269–2281. (k) Wang, S.; Zhang, G.; Zhang, L. *Synlett* **2010**, 692–706. (l) Corma, A.; Leyva-Perez, A.; Sabater, M. J. *Chem. Rev.* **2011**, *111*, 1657–1712. (m) Biannic, B.; Aponick, A. *Eur. J. Org. Chem.* **2011**, 2011, 6605–6617.
- (2) Xiao, J.; Li, X. *Angew. Chem., Int. Ed.* **2011**, *50*, 7226–7236.
- (3) Shapiro, N. D.; Toste, F. D. *J. Am. Chem. Soc.* **2007**, *129*, 4160–4161.
- (4) Li, G.; Zhang, L. *Angew. Chem., Int. Ed.* **2007**, *46*, 5156–5159.
- (5) (a) Davies, P. W.; Albrecht, S. J. C. *Angew. Chem., Int. Ed.* **2009**, *48*, 8372–8375. (b) Davies, P. W. *Pure Appl. Chem.* **2010**, *82*, 1537–1544.
- (6) (a) Yeom, H. S.; Lee, J. E.; Shin, S. *Angew. Chem., Int. Ed.* **2008**, *47*, 7040–7043. (b) Yeom, H. S.; Lee, Y.; Jeong, J.; So, E.; Hwang, S.; Lee, J. E.; Lee, S. S.; Shin, S. *Angew. Chem., Int. Ed.* **2010**, *49*, 1611–1614.

- (7) (a) Cui, L.; Peng, Y.; Zhang, L. *J. Am. Chem. Soc.* **2009**, *131*, 8394–8395. (b) Cui, L.; Zhang, G.; Peng, Y.; Zhang, L. *Org. Lett.* **2009**, *11*, 1225–1228. (c) Cui, L.; Ye, L.; Zhang, L. *Chem. Commun.* **2010**, *46*, 3351–3353.
- (8) (a) Hashmi, A. S.; Bührle, M.; Salathé, R.; Bats, J. *Adv. Synth. Catal.* **2008**, *350*, 2059–2064. (b) Li, C.-W.; Lin, G.-Y.; Liu, R.-S. *Chem.—Eur. J.* **2010**, *16*, 5803–5811.
- (9) Jadhav, A. M.; Bhunia, S.; Liao, H.-Y.; Liu, R.-S. *J. Am. Chem. Soc.* **2011**, *133*, 1769–1771.
- (10) Noey, E. L.; Luo, Y.; Zhang, L.; Houk, K. N. *J. Am. Chem. Soc.* **2012**, *134*, 1078–1084.
- (11) Cuenca, A. B.; Montserai, S.; Hossain, K. M.; Mancha, G.; Lledos, A.; Medio-Simon, M.; Ujaque, G.; Asensio, G. *Org. Lett.* **2009**, *11*, 4906–4909.
- (12) Ye, L.; Cui, L.; Zhang, G.; Zhang, L. *J. Am. Chem. Soc.* **2010**, *132*, 3258–3259.
- (13) Ye, L.; He, W.; Zhang, L. *J. Am. Chem. Soc.* **2010**, *132*, 8550–8551.
- (14) Lu, B.; Li, C.; Zhang, L. *J. Am. Chem. Soc.* **2010**, *132*, 14070–14072.
- (15) He, W.; Li, C.; Zhang, L. *J. Am. Chem. Soc.* **2011**, 8482–8485.
- (16) Ye, L.; He, W.; Zhang, L. *Angew. Chem., Int. Ed.* **2011**, *50*, 3236–3239.
- (17) Wang, Y.; Ji, K.; Lan, S.; Zhang, L. *Angew. Chem., Int. Ed.* **2012**, 1915–1918.
- (18) (a) Bhunia, S.; Ghorpade, S.; Huple, D. B.; Liu, R.-S. *Angew. Chem., Int. Ed.* **2012**, *51*, 2939–2942. (b) Vasu, D.; Hung, H.-H.; Bhunia, S.; Gawade, S. A.; Das, A.; Liu, R.-S. *Angew. Chem., Int. Ed.* **2011**, 6911–6914.
- (19) (a) Pirrung, M. C.; Zhang, J.; Lackey, K.; Sternbach, D. D.; Brown, F. J. *Org. Chem.* **1995**, *60*, 2112–2124. (b) He, W.; Xie, L.; Xu, Y.; Xiang, J.; Zhang, L. *Org. Biomol. Chem.* **2012**, *10*, 3168–3171.
- (20) (a) Fructos, M. R.; Belderrain, T. R.; de Fremont, P.; Scott, N. M.; Nolan, S. P.; Diaz-Requejo, M. M.; Perez, P. J. *Angew. Chem., Int. Ed.* **2005**, *44*, 5284–5288. (b) Fructos, M. R.; de Fremont, P.; Nolan, S. P.; Diaz-Requejo, M. M.; Pérez, P. J. *Organometallics* **2006**, *25*, 2237–2241. (c) Diaz-Requejo, M. M.; Perez, P. J. *Chem. Rev.* **2008**, *108*, 3379–3394. (d) Prieto, A.; Fructos, M. R.; Mar Díaz-Requejo, M.; Pérez, P. J.; Pérez-Galán, P.; Delpont, N.; Echavarren, A. M. *Tetrahedron* **2009**, *65*, 1790–1793.
- (21) Mézailles, N.; Ricard, L.; Gagosz, F. *Org. Lett.* **2005**, *7*, 4133–4136.
- (22) Kirmse, W. *Eur. J. Org. Chem.* **2002**, 2002, 2193–2256.
- (23) Li, G.; Zhang, L. *Angew. Chem., Int. Ed.* **2007**, *46*, 5156–5159.
- (24) Lambert, J. B.; Mueller, P. H.; Gaspar, P. P. *J. Am. Chem. Soc.* **1980**, *102*, 6615–6616.
- (25) (a) Hohenberg, P.; Kohn, W. *Phys. Rev.* **1964**, *136*, B864–B871. (b) Kohn, W.; Sham, L. J. *Phys. Rev.* **1965**, *140*, A1133–A1138.
- (26) Frisch, M. J.; Trucks, G. W.; Schlegel, H. B.; Scuseria, G. E.; Robb, M. A.; Cheeseman, J. R.; Scalmani, G.; Barone, V.; Mennucci, B.; Petersson, G. A.; Nakatsuji, H.; Caricato, M.; Li, X.; Hratchian, H. P.; Izmaylov, A. F.; Bloino, J.; Zheng, G.; Sonnenberg, J. L.; Hada, M.; Ehara, M.; Toyota, K.; Fukuda, R.; Hasegawa, J.; Ishida, M.; Nakajima, T.; Honda, Y.; Kitao, O.; Nakai, H.; Vreven, T.; Montgomery, J. A., Jr.; Peralta, J. E.; Ogliaro, F.; Bearpark, M.; Heyd, J. J.; Brothers, E.; Kudin, K. N.; Staroverov, V. N.; Kobayashi, R.; Normand, J.; Raghavachari, K.; Rendell, A.; Burant, J. C.; Iyengar, S. S.; Tomasi, J.; Cossi, M.; Rega, N.; Millam, J. M.; Klene, M.; Knox, J. E.; Cross, J. B.; Bakken, V.; Adamo, C.; Jaramillo, J.; Gomperts, R.; Stratmann, R. E.; Yazyev, O.; Austin, A. J.; Cammi, R.; Pomelli, C.; Ochterski, J. W.; Martin, R. L.; Morokuma, K.; Zakrzewski, V. G.; Voth, G. A.; Salvador, P.; Dannenberg, J. J.; Dapprich, S.; Daniels, A. D.; Farkas, O.; Foresman, J. B.; Ortiz, J. V.; Cioslowski, J.; Fox, D. J. *Gaussian 09*, revision A.02; Gaussian, Inc.: Wallingford, CT, 2009.
- (27) (a) Perdew, J. P.; Burke, K.; Ernzerhof, M. *Phys. Rev. Lett.* **1996**, *77*, 3865–3868. (b) Perdew, J. P.; Burke, K.; Ernzerhof, M. *Phys. Rev. Lett.* **1997**, *78*, 1396–1396.
- (28) Fuentealba, P.; Preuss, H.; Stoll, H.; Von Szentpály, L. *Chem. Phys. Lett.* **1982**, *89*, 418–422.

- (29) Marenich, A. V.; Cramer, C. J.; Truhlar, D. G. *J. Phys. Chem. B* **2009**, *113*, 6378–6396.
- (30) See Supporting Information for details.
- (31) Benitez, D.; Shapiro, N. D.; Tkatchouk, E.; Wang, Y.; Goddard, W. A., III; Toste, F. D. *Nat. Chem.* **2009**, *1*, 482–486.
- (32) Reed, A. E.; Weinstock, R. B.; Weinhold, F. *J. Chem. Phys.* **1985**, *83*, 735–746.
- (33) Wiberg, K. B. *Tetrahedron* **1968**, *24*, 1083–1096.
- (34) (a) Pyykkö, P. *Angew. Chem., Int. Ed.* **2004**, *43*, 4412–4456.
(b) Pyykkö, P. *Inorg. Chim. Acta* **2005**, *358*, 4113–4130.
- (35) Fang, R.; Yang, L. *Organometallics* **2012**, 3043–3055.
- (36) Correa, A.; Marion, N.; Fensterbank, L.; Malacria, M.; Nolan, S. P.; Cavallo, L. *Angew. Chem., Int. Ed.* **2008**, *47*, 718–721.